Increasing temperature and vapor pressure deficit lead to hydraulic damages in the absence of soil drought

Leonie C. Schönbeck[1,2,3], Philipp Schuler[4,5], Marco M. Lehmann[4], Eugénie Mas[1,2], Laura Mekarni[1,2], Alexandria L. Pivovaroff[6], Pascal Turberg[1,2], Charlotte Grossiord[1,2]

[1] Plant Ecology Research Laboratory PERL, School of Architecture, Civil and Environmental Engineering ENAC, EPFL, CH-1015 Lausanne, Switzerland
[2] Community Ecology Unit, Swiss Federal Institute for Forest, Snow and Landscape WSL, CH-1015 Lausanne, Switzerland
[3] Department of Botany & Plant Sciences, University of California, 2150 Batchelor Hall, Riverside, CA, 92521 USA
[4] Forest dynamics unit, Swiss Federal Institute for Forest, Snow and Landscape WSL, CH-8903 Birmensdorf, Switzerland
[5] Institute of Agricultural Sciences, ETH Zurich, Zurich Switzerland
[6] Biology Division, Glendale Community College, Glendale, CA, 91208, USA

Journal: Plant, Cell and Environment

Figures: 6 (all in color)

Supplementary data: Tables: 3 ; Figures: 6 ; Methods: 1

Keywords: hydraulic conductivity, *Fagus sylvatica,* X-ray micro-CT, PLA, PLC, *Quercus ilex, Quercus pubescens*

Orcid ID

Leonie C. Schönbeck**:** 0000-0001-9576-254X
Philipp Schuler: 0000-0002-5711-2535
Marco M. Lehmann**:** 0000-0003-2962-3351
Alexandria L. Pivovaroff: 0000-0002-3104-1900
Charlotte Grossiord: 0000-0002-9113-3671

Abstract

Temperature (T) and vapor pressure deficit (VPD) are important drivers of plant hydraulic conductivity, growth, mortality, and ecosystem productivity, independently of soil water availability. Our goal was to disentangle the effects of T and VPD on plant hydraulic responses. Young trees of *Fagus sylvatica L., Quercus pubescens Willd.* and *Quercus ilex* L. were exposed to a cross-combination of a T and VPD manipulation under unlimited soil water availability. Stem hydraulic conductivity and leaf-level hydraulic traits (e.g., gas exchange and osmotic adjustment) were tracked over a full growing season. Significant loss of xylem conductive area (PLA) was found in *F. sylvatica* and *Q. pubescens* due to rising VPD and T, but not in *Q. ilex*. Increasing T aggravated the effects of high VPD in *F. sylvatica* only. PLA was driven by maximum hydraulic conductivity and minimum leaf conductance, suggesting that high transpiration and water loss after stomatal closure contributed to plant hydraulic stress. This study shows for the first time that rising VPD and T lead to losses of stem conductivity even when soil water is not limiting, highlighting their rising importance in plant mortality mechanisms in the future.

Introduction

Rising temperatures (T) have caused exponential increases in atmospheric evaporative demand (i.e., vapor pressure deficit, VPD) in many parts of the world (Dai 2006; Grossiord *et al.* 2020a), as the air humidity is not increasing at the same speed as the exponentially rising saturation vapor pressure of the atmosphere. As a result, T and VPD have been identified as increasingly important drivers of plant hydraulic conductivity losses (Olson, Anfodillo, Rosell & Martínez-Méndez 2020), growth reduction (Trotsiuk *et al.* 2021), plant mortality (Adams *et al.* 2009; Allen, Breshears & McDowell 2015) and reduced ecosystem productivity (Ciais *et al.* 2005). Many studies focus on plant responses to a combination of soil drought and either high T ('hot droughts') (Allen *et al.* 2015; Grossiord *et al.* 2018; Cochard 2019; Rehschuh *et al.* 2021), or high VPD (Eamus, Boulain, Cleverly & Breshears 2013; Anderegg & Meinzer 2015; Fontes *et al.* 2018). For example, high VPD combined with soil drought leads to extreme xylem tensions and embolisms (Tardieu & Simonneau 1998). VPD and soil water dynamics are generally closely coupled on timescales from months to seasons (Novick *et al.* 2016; Liu *et al.* 2020), but their individual contributions to plant hydraulics on the timescale from days to weeks are not well established. Disentangling T and VPD under field conditions is challenging because higher T inherently increases VPD (Urban, Ingwers, McGuire & Teskey 2017). As a result, few studies have isolated the physiological effects of rising VPD *vs.* T on plants without soil moisture stress, limiting our ability to anticipate future impacts on terrestrial ecosystems.

Higher VPD enhances the driving force for water loss from the leaves. When the water demand exceeds the supply, the water potential in the leaves and stems becomes more negative, which below a given threshold, can lead to embolisms in the xylem vessels, in turn causing a loss of hydraulic conductivity (K). Due to species differences in vessel pit structure and width, some species are more vulnerable to embolisms than others (Lens *et al.* 2011; Tixier *et al.* 2014). To prevent expensive and sometimes irreparable damages, leaves regulate water loss under high evaporative demand and/or low soil moisture by controlling stomatal opening, thereby regulating leaf and stem water potentials (Martínez-Vilalta, Poyatos, Aguadé, Retana & Mencuccini 2014). With increasing VPD, leaf stomata close gradually (Jarvis & McNaughton 1986; Monteith 1995). Although the exact sensing mechanism involved in stomatal closure to rising VPD is unclear, it is thought to involve changes in the water status in stomatal guard cells mediated by hormonal signals like abscisic acid (Buckley 2005; McAdam & Brodribb 2016). While it is generally thought that stomata close to prevent embolisms, the relationship between the two is still under

discussion, and it is unknown whether and to what extent embolisms may occur before stomata are fully closed (Hochberg *et al.* 2017).

The rate at which stomatal closure occurs, i.e., the stomatal sensitivity to VPD (*m*), differs per species and along climatic gradients, with plants adapted to more xeric biomes having lower stomatal sensitivity to changes in VPD (i.e., stomata close more slowly) than those adapted to mesic ones (Martínez-Vilalta *et al.* 2014; Novick *et al.* 2016). Yet, how stomatal sensitivity variation between xeric and mesic species alters hydraulic damages without soil moisture limitation remains unclear. Moreover, stomatal sensitivity can be adjusted in response to enduring environmental stress. For instance, Cardoso *et al*. (2020) showed that stomatal closure in response to VPD was delayed in plants with lowered leaf osmotic potential. This reduction in osmotic potential is achieved, among others, by accumulating soluble sugars in the cells, which lowers the turgor loss point (ψ_{TLP}), i.e., the leaf water potential below which the cells lose turgor and start to wilt. Such a response would allow extended stomatal opening and higher water losses before risking hydraulic failure under high VPD, thereby benefiting carbon assimilation. However, while adjustment of osmotic potential has been documented in roots and leaves in response to soil drought (Schönbeck *et al.* 2018), it is unknown whether similar mechanisms occur in response to high VPD and/or T under ample water supply.

Even after stomatal closure, water loss continues through incompletely closed stomata and the cuticle (i.e., minimum leaf conductance, g_{min}) (Duursma *et al.* 2019), representing a significant risk for plants, particularly in the context of rising VPD. The cuticle, meant to serve as a protective leaf shield against water loss, pathogens, and UV damage (Kerstiens 1996; Schuster, Burghardt & Riederer 2017), still provides a significant alternative pathway for water to exit the leaf, with its conductance even exceeding that of leaky stomata (Gardingen & Grace 1992). The mechanisms behind g_{min} and the role of the cuticle are still poorly understood, as are the responses of g_{min} to environmental changes. A reduction in g_{min} was observed in response to soil drought and increasing VPD (Bengtson, Larsson & Liljenberg 1978; Gardingen & Grace 1992; Drake *et al.* 2018). In response to high T, both steep increases of g_{min} (Schuster *et al.* 2016) and reduction due to long-term heat stress have been demonstrated (Duursma *et al.* 2019). Nevertheless, the possible prominent role of g_{min} in total water loss indicates that the mechanism must be considered a final step to plant desiccation under plant stress conditions.

In addition to leaf hydraulic properties, leaf T control is essential to maintain photosynthetic capacity under high T because biochemical processes like photosynthesis and respiration have a certain T optimum, below and above which these enzymatic processes slow down (Berry & Bjorkman 1980). Higher

T can induce stomatal opening to provide leaf cooling by evaporation (Urban *et al.* 2017), and may thus induce opposite effects to high VPD. Thermal tolerance, i.e., the ability to photosynthesize under a specific high T (Seemann, Berry & Downton 1984), might be strongly connected to plant hydraulics and drought tolerance (Knight & Ackerly 2002; Gimeno, Pías, Lemos-Filho & Valladares 2009), with low thermal tolerance requiring more leaf cooling and resulting in a high water demand under warm conditions. Xeric species adapted to dry conditions may thus have the possibility for stronger leaf cooling without risking hydraulic failure compared to mesic species (Urban *et al.* 2017). Higher T also decreases water viscosity, allowing higher leaf transpiration rates and possibly exerting more substantial reductions in leaf and stem water potential in addition to high VPD (Cochard, Martin, Gross & Bogeat-Triboulot 2000b; Yang, Zhang, Huang, Peng & Li 2020).

In this study, our goal was to disentangle the effects of T and VPD on plant hydraulic responses. We exposed well-watered young trees from *Fagus sylvatica L., Quercus pubescens Willd.* and *Quercus ilex*, three species differing in hydraulic safety strategies (Table S1 & Fig. S1), to a cross-combination of a T and VPD manipulation under unlimited soil water availability. We tracked the response of stem hydraulic conductivity and the leaf-level mechanisms that may drive the loss of conductivity (g_s, m, g_{min}, ψ_{leaf}, ψ_{TLP}, leaf sugar concentrations). Specifically, we investigated whether increasing T and VPD would induce hydraulic stress in the form of a higher percentage loss of conductive area (PLA, %) of the stem xylem. We used micro-computed tomography (µCT) to determine PLA and confirmed the method with pressure-flow techniques to assess loss of hydraulic conductance (PLC, %) (Sperry, Donnelly & Tyree 1988). We compared PLA responses with a range of plant traits (g_s, g_{min}, K_s leaf sugar concentrations, and ψ_{TLP}) to find potential drivers of PLA among all three species. We hypothesized that 1) increasing VPD, independent of T changes and in the absence of soil drought, causes tension on the hydraulic transport system as long as stomata remain open by reducing leaf water potential and inducing loss of xylem conductivity (PLC and PLA) with mesic species being more strongly affected than xeric ones; 2) higher T alone leads to higher foliar transpiration (and little to no stomatal regulation) thereby supporting leaf cooling but causing an aggravating effect on the loss of conductivity in combination with increasing VPD, especially in mesic species with a lower T optimum.

Materials and methods

Species and experimental setup

Three ecologically and hydraulically contrasting tree species relevant to a wide range of European forest ecosystems were selected for the experiment. On a gradient from mesic to xeric species, these are: the

maritime-temperate European beech (*Fagus sylvatica L.*, provenance Biberist, Switzerland, 440-490 m asl), the sub-Mediterranean pubescent oak (*Quercus pubescens Willd.*, provenance Leuk, Switzerland, 720-750 m asl), and the Mediterranean holm oak (*Quercus ilex*, provenance Veneto region, Italy, 0-50 m asl) (Fig. S1, Table S1 for ψ_{TLP}, K_{max} and ψ_{P50}). In March 2020, 108 even-sized three-year-old trees per species were planted from quick-pots into 3 L pots filled with water-retaining soil (40% clay, 25% bark compost, 20% broken puffed clay, 15% peat replacement from wood fibers; Kübelpflanzenerde, RICOTER Erdaufbereitung AG, Aarberg, Switzerland). Quick-pots are tree propagation trays (650 cm^3) which allow the roots to stay connected to the soil and not to be disturbed during transplanting. This study used six climate chambers (PGV36, Conviron, Winnipeg, Canada) at the Phytotron facility of ETH, Zürich, Switzerland, to manipulate air T and VPD using a factorial design, each housing 18 individuals per species. The light roofs of the climate chambers were adjusted in height so that light intensity at canopy height was in all chambers ~390 µmol m^{-2} s^{-1}. At this light intensity, all three species are at, or approach their light saturation point (Staudt, Joffre & Rambal 2003; Pena-Rojas, Aranda & Fleck 2004; Čater & Kobler 2017; Petersson, Löf, Jensen, Chastain & Gardiner 2020). All plants were regularly (i.e., every two to three days) watered by hand to ensure complete soil hydration, and soil volumetric water content (VWC) was manually measured bi-weekly to ensure no soil drought occurred (Fig. S2).

Due to a lockdown during the global pandemic of 2020, the plants were kept in a cool climate chamber (4°C) with 6 hours of daylength during March and April 2020 to delay bud break until access to the climate chambers was possible in May 2020. The plants were first exposed to an acclimation period of five weeks to recover from the transport and leaf flush inside the climate chambers. During this period, all chambers were set to 16 daylight hours, T of 25°C, and relative humidity (RH) of 50%. Nighttime was six hours long with a T of 15°C and RH of 50%. One-hour dawn and dusk occurred between day and night. Air T and humidity were continuously (10 min resolution) measured at canopy height in each chamber with Onset HOBO MX T and RH loggers (Onset computer corporation, Bourne MA, USA).

After the acclimation period, three chambers were set to daytime T of 25°C and three to 30°C. Nighttime T was set to 10°C lower than during the day in all chambers (i.e., 15 and 20°C). Within every T group, chambers were given a low (1 kPa ± 0.3), medium (1.6 kPa ± 0.3), or high (2.2 kPa ± 0.3) daytime VPD treatment by setting RH to reach the desired VPD levels. The highest VPD level was selected based on the physical limitations of the climate chambers to reach a maximum temperature of 30°C and the minimum RH that could be reached with the addition of a dehumidifier. While a VPD of 2.2 kPa is not excessive compared to what the xeric species in this study experience during the dry season in their natural habitat

(Tognetti, Longobucco, Miglietta & Raschi 1998a), we do believe the range of VPD was sufficient to induce plant hydraulic changes. Because of difficulties in regulating humidity levels in the chambers, RH was kept similar during day and night, even though such conditions are unlikely in real-world conditions. The goal RH was calculated by solving the equation for VPD using the Tetens formula (Monteith & Unsworth 2013). VPD was calculated as the difference between saturated and actual VPD:

$$actual\ VPD = \frac{(RH * VP_{sat})}{100} \quad (1),$$

$$VP_{sat} = 0.6108 * e^{\frac{17.27*T}{T+237.3}} \quad (2),$$

where VP_{sat} is saturated VP at a given T in °C.

A humidifier was added to the chamber with 30°C + low VPD (to reach 78% RH), and dehumidifiers were used to increase VPD as high as possible in the 25°C and 30°C chambers + high VPD. While all chambers maintained stable T throughout the experiment, the difficulty in manipulating air humidity in the chambers led to slight VPD variation over time (Fig. S2). Despite this, VPD levels were consistently within the set range (0.7 – 1.3 kPa for low, 1.3 – 1.9 kPa for medium, and 1.9 – 2.5 kPa for high VPD) (Figs. 1 & S2).

Six plants per chamber and species were randomly selected for repeated physiological measurements. The physiological measurements were carried out during four campaigns that were held at a ~5-week interval, with the first campaign just before the start of the treatments: 1-10 June (campaign 1, pre-treatment); 13-23 July (campaign 2, + 5 weeks); 26 Aug-4 Sep (campaign 3, + 10 weeks); and 19 -31 Oct (campaign 4, +15 weeks). Across all campaigns, physiological measurements were performed on the same leaf of each individual, unless the leaf wilted or dropped. During each campaign (apart from campaign 3), six randomly selected individuals per chamber and species were harvested for destructive measurements as described below (Fig. S3). The individuals used for physiological measurements were harvested during the last campaign.

Stomatal conductance and VPD response

Stomatal conductance (g_s, mmol m^{-2} s^{-1}) and transpiration (E, mmol m^{-2} s^{-1}) were measured on each tree selected for repeated physiological measurements (6 replicates per species) during each campaign using four LiCor LI-6800 (LiCor Inc., Lincoln, Nebraska, USA). One leaf was clipped in the cuvette, set to ambient chamber T and RH, with a light intensity of 1500 µmol m^{-2} s^{-1} PAR and flow at 500 µmol s^{-1}. While 1500 µmol m^{-2} s^{-1} is well above the ambient light conditions in the chambers, using this standard light value

during gas exchange measurements ensures cross-comparison with other studies and light-saturation of the trees. The leaf was left acclimating for 20 minutes or longer if needed to reach stable g_s. The g_s at 400 ppm CO_2 was extracted from photosynthesis over CO_2 (A/C_i) measurements, including three log entries at 400 ppm CO_2. The three measurements were then averaged.

Response curves of g_s to VPD variation were measured on five replicates per species by measuring g_s at 75, 60, 45, 30, 15, and 5% RH, with similar light, CO_2, T, and flow as described above. RH was chosen to vary instead of VPD to ensure that the VPD would be solely controlled by RH in the LiCor instrument. Each step included a minimum waiting time of 15 minutes for *F. sylvatica* and 20 minutes for both *Quercus* species to allow for g_s stabilization between each RH step. *F. sylvatica* reached stable g_s faster than the two *Quercus* species. In the chambers with the highest VPD (i.e., lowest humidity), the LiCor devices did not always reach 75% RH. Nonetheless, all g_s to VPD curves started at VPD values <1.1 kPa. The reference g_s at 1 kPa VPD ($g_{s,ref}$, mmol m^{-2} s^{-1}) and the stomatal sensitivity (m, mmol m^{-2} s^{-1} kPa^{-1}) of each tree and each campaign was extracted by fitting logarithmic curves to the data (for detailed curve fitting methods, see Methods S1, Figs. S4 & S5):

$$g_s = -m \times \log(\mathrm{VPD}) + g_{s,ref} \qquad (3)$$

The curve fits resulted in an m to $g_{s,ref}$ ratio of 0.46, which is slightly lower but close to the suggested ratio of 0.5-0.6 suggested by Oren *et al.* (1999) (Fig. S5). The g_s to VPD response curves differ from the point measurements in the climate chambers at the ambient VPD levels. The VPD response curves represent the response to rapid changes in VPD (over 2h), while the point measurements represent the long-term acclimation of g_s to different VPD levels. In addition, the VPD response curves were done over a more extensive range of VPD levels (0.8-3.5 kPa) than the chambers could reach (1 -2.2 kPa) (see also Methods S1).

Minimum leaf conductance (g_{min})

Minimum leaf conductance (Kerstiens 1996) was measured as described in Pearcy & Zimmermann (2000). One leaf per individual was cut before dawn when stomata were assumed to be still closed. The cut petiole was immediately sealed with melted candle wax, and the leaf area was scanned using a flatbed scanner, followed by analysis using Pixstat (Schleppi 2021). The leaves were stuck to a lab tape run between two lab stands, standing in a small dark climate chamber with stable T (26°C) and humidity (60%) and the ventilation on. Every 15-20 minutes, the leaves were taken from the climate chamber and weighed in a dark room using a fine-precision scale (Mettler-Toledo, Cole-Palmer, Illinois, USA). This procedure was

repeated eight times. g_{min} (mmol m^{-2} s^{-1}) was calculated as cuticular transpiration per mole fraction VPD, assuming the leaf internal air to be fully saturated (Pearcy *et al.* 2000).

Pressure volume curves and leaf water potential at predawn and midday

Pressure-volume curves were determined using the bench-dehydration method (Koide, Robichaux, Morse & Smith 2000). Before dawn, a leaf from the top of the crown was cut off and immediately sealed in a plastic bag (Whirlpak) that was previously exhaled in. Predawn water potential (kPa) was measured directly using a Scholander-type pressure chamber (PMS Instrument Company, Model 1505D, Albany, OR, USA). The same leaf was immediately weighed using a fine-precision scale (Mettler-Toledo), placed in a plastic bag, and allowed to dry progressively in the open plastic bag on a lab bench. The procedure of measuring water potential, weighing, and drying was repeated with increasing drying time intervals (from 10 s to 1 h) for the two *Quercus* species until achieving water potentials of about -4 MPa or until water potential reached a plateau. For *Fagus sylvatica*, the procedure was repeated continuously without letting the leaves dry on the bench due to the rapid water loss and a corresponding drop in leaf water potential. Subsequently, the leaves were individually put in a paper bag and dried in an oven at 60°C for 24 h to determine the dry mass. Leaf water potential at turgor loss point (Ψ_{TLP}, MPa) was calculated after Koide *et al.* (2000). At midday, another leaf was cut off from the same individuals, and midday water potential (Ψ_{md}) was measured.

Percent loss of conductive area

On the three harvest dates (June, July, and October), six trees per chamber and species were transported to the Interdisciplinary Platform for X-ray micro-computed tomography (µCT) (PIXE, EPFL, Lausanne, Switzerland) and stored in a cool room in the absence of direct light (to avoid transpirational water loss), until they were scanned. For the µCT scanning, the tree was fixed in a custom-built plant holder, and its branches were wrapped in cling film to prevent movements during the measurements that could alter the quality of the images. A 1 cm part of the stem to be scanned at approximately 40 cm height was marked with tape before starting the measurements. The tree was then moved onto the scanning platform and scanned at 80 keV and 87uA in the RX-Solutions Ultratom X-ray scanner using a Hamamatsu 230 kV X-ray tube in reflection mode. The sapling rotated in 0.22° increments during the scan, yielding between 1400-1600 two-dimensional projections with a ~5-7 micrometer pixel resolution. The acquired longitudinal projections were reconstructed (Filtered backprojection) into a “stack” of multiple transverses TIF images using Xact (RX-Solutions, version 2.0 R9901). After scanning, the scanned part of the stem was cut and

252 flushed with 1 bar air pressure for 1.5 min and subsequently scanned again to obtain a fully embolized
253 stem cross-section as a reference that allowed us to visualize all vessels in the sapwood (Fig. 2).

254 Image analysis was done with the Avizo software (2019.4). The assessment was done on one image
255 located in the middle of the scanned volume, as we found no significant differences between the bottom,
256 top, and middle of the 1 cm stem portion during preliminary tests. The area of interest was selected by
257 excluding bark and phloem (Fig. 2). Segmentation was performed by defining a selection threshold such
258 that most of the air around the stem was chosen as a reference, without including any material on the
259 bark and making sure that the concurrently selected void vessels did not merge due to a wide selection
260 range. A visual assessment of each scan followed the automated threshold tool segmentation to assess
261 scan quality, artifacts, and white level. Percent loss of conductive area (PLA, %) was calculated as the total
262 embolized area in the intact stem divided by the total vessel area in the flushed stem (x100%). Due to
263 flushing, some stem samples had shrunk. A correction factor was used to control the stem area of the
264 shrunk sample. To estimate the impact of the treatments over time, we used the average PLA per species
265 and chamber from the first harvest (i.e., to account for potential cavitation present before the treatments
266 started) and deducted these values from the results of the second and third harvest (dPLA, %.).

267 *Percent loss of conductivity*

268 On the last harvest, after the trees were scanned by the µCT, the stem was cut immediately above the
269 scanned part to measure the hydraulic conductivity. These measurements were done to confirm the
270 methodology and results of the µCT scans. Hydraulic conductivity (K, kg m s^{-1} MPa^{-1}) was measured using
271 a commercial XYL'EM Plus apparatus (Bronkhorst, Montigny-les-Cormeilles, France) according to the
272 method described by Sperry *et al.* (1988). The branch was recut underwater and left in the water for at
273 least 30 minutes to relax xylem tension in the branch segment. The segment was then cut to its final size.
274 Its proximal end was connected to the tubing system of the XYL'EM, which was filled with deionized
275 filtered and degassed water with 10mM KCl and 1mM $CaCl_2$, flowing from an elevated source. Initial
276 hydraulic conductivity (K_i, kg m s^{-1} MPa^{-1}) was recorded. The stem segment was then flushed with water
277 at 1.5 bar for 1 min to remove emboli, and its maximum hydraulic conductivity (K_{max}, kg m s^{-1} MPa^{-1}) was
278 measured. A second flush at 1.5 bar for 30 s followed by a measurement was done to confirm the
279 maximum hydraulic conductivity value. Percentage loss of conductivity (PLC, %), a direct estimate of the
280 percentage of embolized vessels (Cochard, Bodet, Améglio & Cruiziat 2000a), was calculated as

281 $$PLC\ (\%) = \frac{K_m - K_i}{K_m} \times 100\%$$

Leaf sugar concentrations

At each destructive sampling campaign (i.e., first, second and last campaign), four leaves per individual were dried in an oven at 60°C until reaching stable weight. The leaf material was homogenized with a ball mill. Sugar concentrations were determined with an enzymatic extraction method described by (Wong 1990) and adapted according to (Hoch, Popp & Körner 2002). The sugars measured using this method are defined as low molecular weight sugars (glucose, fructose, and sucrose). 10-12 mg of ground material was boiled in 2 ml distilled water for 30 minutes. After centrifugation, an aliquot of 200 µl was treated with Invertase and Isomerase from baker's yeast (Sigma-Aldrich, St. Louis, MO, USA) to degrade sucrose and convert fructose into glucose. The total amount of glucose (sugars) was determined photometrically at 340 nm in a 96-well microplate photometer (HR 7000, Hamilton, Reno, NE, USA) after enzymatic conversion to gluconate-6-phosphate (hexokinase reaction, hexokinase from Sigma Diagnostics, St. Louis, MO, USA). Pure glucose-, fructose- and sucrose- solutions were used as standards, and standard plant powder (Orchard leaves, Leco, St. Joseph, MI, USA) was included to control the reproducibility of the extraction. Sugar concentrations are expressed on a percent dry matter basis. Because all samples were run in a single laboratory with no change in protocol during the processing, issues with comparing results across methods or labs were obviated (Quentin *et al.* 2015).

Statistical analysis

The similarities between PLA and PLC measurements were tested by fitting a linear model to the data with PLA explaining PLC. If the confidence interval of the slope includes 1, a 1:1 relationship between PLA and PLC is assumed.

Treatment differences

Data were analyzed for each species separately. A mixed-effect model was carried out for each parameter (excl. dPLA and PLC, see below) with T, VPD, and campaign (only the three measurement campaigns after the start of treatment) as fixed factors, including all interactions while controlling for repeated measures on the tree individual (included as a random factor). The model was then analyzed using a type-3 ANOVA using Satterthwaite's estimation. The timepoint did not show any significant interactions with the treatments. Thus, it was decided to pool all data of the three campaigns. A two-way ANOVA without mixed effects (no repeated measurements) was used for dPLA and PLC, with T and VPD, including their interaction, as explanatory variables.

Correlations between plant physiological parameters

To relate PLA to different leaf-level hydraulic characteristics that may drive the loss of conductivity, correlation analyses were carried out for PLA paired with all other parameters: E, g_s, g_{min}, m, ψ_{TLP}, ψ_{midday}, $K_{s,max,}$ and sugar concentration in the leaves. Data for all species were pooled. For significant correlations ($p < 0.05$), the parameters were plotted, and a regression line was added to illustrate the relationship between the two.

Results

Correlation between PLA and PLC

The percent loss of conductivity (PLC, %) measured with the pressure-flow technique and the percent loss of conductive area (PLA, %) measured using µCT were strongly correlated (Fig. 3). The regression line did not significantly deviate from the 1:1 line, indicating the µCT method is reliable and comparable to the pressure-flow technique (Nolf *et al.* 2017). We will focus mainly on the PLA results in the following sections because PLC was only measured in the last campaign, while PLA was measured during three campaigns.

VPD and T effects on plant hydraulics

***F. sylvatica**:* Increased VPD and T significantly raised the loss of hydraulic conductance (dPLA, the difference between pre-treatment and during-treatment PLA, and PLC) in *F. sylvatica* (Fig. 4, Table S2). High VPD caused a decrease in $\psi_{leaf,pd}$, $\psi_{leaf,md,}$ and g_{min} (Figs. 4 & 5, Table S2 & S3), but the latter only in the 30°C chambers. Higher T reduced $\psi_{leaf,md,}$ and interacted with VPD, causing even stronger reductions of $\psi_{leaf,md}$ with higher VPD. Transpiration (E) increased with rising VPD, but no effect of T was observed. T but not VPD was found to affect stomatal sensitivity (*m*), where *m* was higher at 30°C than at 25°C. No impact of T or VPD was seen on ψ_{TLP} and g_s, although a decreasing trend with higher VPD was visible for the latter.

***Q. pubescens**:* dPLA increased with rising VPD in *Q. pubescens* and was lower at 30°C than 25°C (Fig. 4, Table S2). No treatment effects were found for PLC. Higher VPD caused an increase in E and a reduction in $\psi_{leaf,md,}$ and ψ_{TLP}. An interaction between T and VPD affected ψ_{TLP}, where ψ_{TLP} decreased with higher VPD only in the 30°C chambers (Fig. 5, Table S3). *m* was higher and $\psi_{leaf,pd}$ was lower at 30°C than at 25°C (Figs. 4 & 5). No VPD or T effects were found for $g_{s,}$ or g_{min} (Fig. 5).

Q. ilex: VPD did not affect either dPLA or PLC (Fig. 4, Table S2), nor E, *m,* $g_{s,}$ or g_{min} (Fig. 5, Table S3). g_{min} and $\psi_{leaf,pd}$ were slightly lower in the 30°C than the 25°C chambers. As for *Q. pubescens,* ψ_{TLP} decreased with increasing VPD but only in the 30°C chambers (Fig. 5, Table S3).

Correlation between PLA and leaf traits

Across all species, PLA was positively correlated with g_{min}, $K_{max,}$ and sugar concentrations in the leaves, indicating that higher water transport rates, evaporative water loss, and osmotic potential were related to higher embolism rates (Fig. 6). However, the correlations between PLA and K_{max} or sugar concentrations were only found in the 30°C treatments, suggesting that enhanced water transport (potentially leading to higher E) and osmotic potential (potentially delaying stomatal closure) only drive increased PLA when the temperature is high. In addition, more negative $\psi_{leaf,md}$ were correlated to higher PLA, but only in the 30°C chambers, indicating that higher tension within the conductive leaf tissues (because of sustained stomatal opening) translated to higher levels of stem xylem embolism (Fig. 6). No correlation was found between PLA and g_s, *m* and ψ_{TLP}

Discussion

Effects of increasing VPD and temperature on the plant hydraulic system in the absence of soil drought

For the first time, we disentangled the effects of temperature (T), vapor pressure deficit (VPD), and their interactions in the absence of soil drought on plant hydraulic traits. Doing so is rare due to the tight relationship between T and VPD in nature. We show that rising T and VPD can cause major hydraulic dysfunctions in trees without soil drought. This was demonstrated by the significant loss of xylem conductive area and conductivity (PLA and PLC, respectively) in *F. sylvatica* and *Q. pubescens* and the increasingly negative leaf water potential ($\psi_{leaf,md}$) in all species with increasing VPD and T (Fig. 4). Considering that this study covered only one growing season and that VPD and T levels were moderate compared to the extreme conditions that occur in nature (e.g., the 2018 hot drought in Europe) (Fu *et al.* 2020; Senf & Seidl 2021), these results highlight the severe threat that chronic VPD and T rise pose on mesic trees, even without any changes in precipitation. Given the high reliability of T predictions in climate models, compared to the uncertainties associated with precipitation (IPCC 2021), these results are particularly relevant for modeling forest ecosystem functioning. While understanding how VPD and T affect plant function is fundamental, it is important to note that our experimental design limits our ability to extend these results to real-world implications. In the field, elevated VPD for several weeks would most likely lead to reduced soil moisture.

We expected to see an increasing gradient in PLA from xeric towards mesic species in response to rising T and VPD, due to differing hydraulic strategies and adaptations (Meyer, Buras, Rammig & Zang 2020), with more extensive T and VPD effects on mesic *F. sylvatica* than the rather xeric *Q. pubescens* and *Q. ilex*. Indeed, 30°C and high VPD (2.2 kPa) exposed *F. sylvatica* to ψ_{leaf} close to its turgor loss point (-2 MPa, Figs. 4 & 5, Table S1). Combined with barely declining g_s and no change in sugar concentration, the absence of

373 stomatal closure and osmotic adjustments increased PLA and PLC. Our results correspond to earlier
374 findings where VPD levels as low as 1.4 kPa caused biomass and ψ_{leaf} reduction in *F. sylvatica* (Lendzion &
375 Leuschner 2008). Moreover, the lack of leaf-level acclimation (e.g., stomatal closure or adjustment of
376 turgor loss point) was previously observed in *F. sylvatica* during soil drought (Backes & Leuschner 2000;
377 Thomas 2000; Schipka, Heimann & Leuschner 2005; Pflug *et al.* 2018). Our observations that transpiration
378 (E) continues even at high levels of embolism (Fig. 5) were confirmed in adult *F. sylvatica* trees in
379 Switzerland (Walthert *et al.* 2021). In this study, the authors further suggested that *F. sylvatica* does not
380 prevent water loss and embolism by leaf physiological acclimation or shedding but sheds its leaves only
381 after embolism has occurred (Walthert *et al.* 2021). Recently, Zhu *et al.* (2022) showed how *F. sylvatica*
382 leaf traits were driven by previous years' VPD over a record of 25 years, suggesting a strategy of leaf
383 shedding and regrowth rather than acclimation during the current year. Overall, our work indicates that
384 the strategy of *F. sylvatica* results in a high risk for hydraulic failure under moderate atmospheric stress
385 (Burkhardt & Pariyar 2016). Together with the slow recovery capability of this species after stress
386 exposure (Hacke & Sauter 1996), these findings highlight its high sensitivity to projected climate (Dittmar,
387 Zech & Elling 2003; Geßler, Keitel, Nahm & Rennenberg 2004).

388 For *Q. pubescens*, PLA increased with rising VPD, although it was generally lower than in *F. sylvatica.*
389 $\psi_{leaf,md}$ did not reach values lower than -1 MPa, indicating a reduced T and VPD impact on the hydraulic
390 system compared to *F. sylvatica*. In contrast to *F. sylvatica,* where no physiological adjustment to rising
391 VPD and T was found*, Q. pubescens* lowered its ψ_{TLP} to withstand more negative leaf water potentials and
392 sustain high g_s and E under rising T and VPD. These results indicate a more conservative water use strategy
393 than *F. sylvatica*. *Q. pubescens* is one of the most widespread species in southern Europe and is known
394 for its high thermal tolerance and drought resistance (Wellstein & Spada 2015). Previous studies showed
395 that this species is well protected against heat-induced perturbations (Haldimann & Feller 2004). Yet, our
396 work suggests that rising T and VPD levels, even moderate ones that this species is frequently exposed to
397 in nature, could, to some extent, negatively impact the efficiency of the hydraulic system. Here we wanted
398 to expose different tree species to comparable T and VPD levels to assess species sensitivities. Still, to
399 better understand VPD and T effects in real-world conditions, future work should focus on extreme
400 conditions that southern tree populations are more likely to experience.

401 Variation between the two xeric *Quercus* species was expected due to their contrasting leaf habit
402 (deciduous *vs*. evergreen) and xylem conduit size (ring-porous vs. diffuse-porous) (Tognetti, Longobucco
403 & Raschi 1998b). PLA and PLC of *Q. ilex* were, in contrast to *Q. pubescens*, not affected by VPD and T,

confirming the low sensitivity of this species to VPD and T, partially due to its smaller, diffuse-porous vessels. This Mediterranean species is highly adapted to dry environments (Barbero, Loisel & Quézel 1992), and the T and VPD levels it was exposed to are likely far from its thermal and hydraulic limits (Fig. S1, Table S1). Moreover, with its tough, evergreen leaves, it reaches photosynthetic efficiency both in cool winter T and dry summers, demonstrating adaptation of the species to a range of extreme conditions far from our experiment (García-Plazaola, Artetxe & Becerril 1999). Its physiological plasticity was shown by reducing g_{min} and ψ_{TLP} in response to increasing T and VPD, respectively, even if these had no impact on PLA. The strong response to these relatively minor changes confirms the rather drought-avoiding behavior of the species (Gullo & Salleo 1990).

Mechanisms driving PLA

We expected significant leaf-level adjustments in response to VPD and T and a correlation between the leaf-level responses and PLA. These relationships would help identify underlying drivers of hydraulic conductivity changes. Increasing VPD led to higher leaf-level transpiration (E, Fig. 5). Still, against our expectations, stomatal conductance and the stomatal sensitivity to VPD (*m*) showed the most negligible response to T and VPD, neither were they, nor E correlated with PLA (Fig. 6). A reason for the absence of stomatal response (g_s and *m*) to VPD and T in all species might be a combination of the choice of species and the level of evaporative demand in the climate chambers. In the case of *F. sylvatica*, a moderate increase in VPD in the absence of soil drought didn't lead to stomatal closure but enhanced E, thereby creating tensions within the xylem that sustained embolism formation. The strategies discussed for *F. sylvatica* point to a risk-taking strategy where leaf shedding due to stress would be more likely than stomatal closure to prevent embolisms (Walthert *et al.* 2021). In contrast, *Q. pubescens* and *Q. ilex* kept their stomates open at the VPD levels in our chambers, but ψ_{leaf} was not sufficiently low to induce embolism. These findings shed new insights into the sequence of hydraulic shutdown in plants. The sequence of stomatal closure, turgor loss, and loss of xylem conductivity have been studied thoroughly in relation to soil drought, where the ψ_{leaf} is a leading indicator for the occurrence of leaf and wood hydraulic pathway failures (Bartlett, Klein, Jansen, Choat & Sack 2016). These findings suggest that 50% PLC approximately coincides with the point where g_s decreases by 95% (ψ_{gs95}), indicating a strong correlation between g_s and PLC. In our study, we could not confirm the strong correlation between hydraulic conductance and g_s, suggesting different pathways in response to atmospheric drought compared to soil drought.

Minimum leaf conductance (g_{min}) was positively correlated with PLA across all species (Fig. 6), indicating that plants or species with higher evaporative water loss would have a higher risk for embolisms under rising VPD and T. Interestingly, with increasing T, this correlation was even steeper. g_{min} has long been considered an insignificant factor in crop drought resistance (Kerstiens 1996). However, recent studies provide evidence that g_{min} may be the last hurdle before dehydration, thereby playing a much more important role than previously thought (Duursma *et al.* 2019). Here we show that g_{min} might be responsible for increased cavitation risk under high VPD, T, and non-limiting soil moisture conditions. The PLA effect of g_{min} might have been exacerbated by the relatively high nighttime VPD levels in our experiment (Fig. S2), compared to natural conditions where relative humidity often approaches 100% during the night. The relatively high VPD and residual water loss from the leaves caused lowered predawn water potentials in *F. sylvatica* even though the soil was fully hydrated (Fig. 4). In *F. sylvatica* and *Q. pubescens*, g_{min} rates were approximately 10% of the g_s values (Fig. 5), indicating a significant water loss at night or when stomata close. The capability to adjust g_{min} in response to a changing environment could be advantageous for protecting valuable xylem vessels. g_{min} reduction was indeed observed in *F. sylvatica* and *Q. ilex* in response to increasing T and VPD, or T only, respectively (Fig. 5), suggesting lower residual water loss in warmer and drier conditions. These results correspond with other studies that have shown a decrease in g_{min} in response to higher evaporative demand (Fanourakis, Heuvelink & Carvalho 2013). It is unknown whether g_{min} changes are caused by the altered chemical composition of the cuticle, increased cuticle deposition, or changing stomatal anatomy in the longer term (Duursma *et al.* 2019). The relationship between g_{min} and T turns out to be even more complex: rapid increases of g_{min} were observed in response to increasing T (Schuster *et al.* 2016; Drake *et al.* 2018), but a negative relationship was found between thermal tolerance and g_{min} (Schuster 2016), indicating that acclimation to increasing T leads to lower g_{min}. However, g_{min} adjustments in *F. sylvatica* were insufficient in our study to prevent plant dehydration and increase PLA under moderately rising VPD.

Higher PLA was also associated with higher maximum stem hydraulic conductance (K_{max}) across species, supporting previous work that reported increased risk for embolisms with higher water transport capacity (Tognetti *et al.* 1998b). There was a gradient in K_{max} between *F. sylvatica*, *Q. pubescens,* and *Q. ilex* (0.014, 0.013, 0.007 kg m s^{-1} MPa^{-1} resp.), in line with the degree of PLA over those three species (Table S1, Fig. S6). These results correspond to the safety-efficiency trade-off (Grossiord, Ulrich & Vilagrosa 2020b), whereby high K_{max} provides fast and efficient water transport but with an increased risk of embolism even in the absence of soil moisture stress. The strongest correlation between PLA and K_{max} in the 30°C

chambers could be explained by the lower water viscosity at warmer T, as higher water transport rates could lead to faster dehydration and increased PLA (Cochard *et al.* 2000b).

Interestingly, leaf sugar concentration was also positively correlated with PLA. VPD and T effects were only found on sugar concentrations of *Q. pubescens* (Fig. S6). Increasing T resulted in higher leaf sugar concentrations, probably due to rising assimilation rates as T optima for temperate European *Quercus* species can reach up to ~30-35°C (Daas, Montpied, Hanchi & Dreyer 2008). In contrast, higher VPD resulted in a minor but significant reduction of sugar concentration in the leaves of *Q. pubescens,* thereby reducing the osmotic potential. Trees tend to accumulate sugars in leaves and roots, lower the turgor loss point, and increase the water holding capacity in response to soil drought (Schönbeck *et al.* 2018). Although for *Quercus* species*,* an adjustment of ψ_{TLP} was observed, the reduced sugar concentrations suggest that other chemical compounds might be responsible for the reduction in ψ_{TLP}.

The individual role of T and VPD on plant hydraulics

The aggravating effect of T in interaction with VPD, mainly in *F. sylvatica*, suggests that T and VPD play independent roles in affecting plant hydraulics. However, VPD seems to be the stronger driver of plant hydraulics. PLA, PLC, ψ_{leaf}, E, $g_{min,}$ and ψ_{TLP} were all affected by VPD in one or more species. On the other hand, T appears to aggravate VPD effects (for $\psi_{leaf,}$ g_{min}, ψ_{TLP}) while only acting independently towards PLA and *m* (Figs. 4 & 5). Earlier studies confirm that higher T can aggravate the adverse effects of increasing VPD (Barron-Gafford, Grieve & Murthy 2007), as physiological controls for water transport become less effective at higher T (Sermons, Seversike, Sinclair, Fiscus & Rufty 2012). The relationship between T and plant hydraulics is complex and partly indirect: T increases E (Urban *et al.* 2017), thereby providing leaf cooling in warmer climates. However, against expectation, we did not find an individual role for T in affecting E (Fig. 5). This finding indicates that 30°C was insufficient to induce active leaf cooling.

Conclusion

For the first time, we show that rising VPD and T can lead to stem conductivity losses even when soil water is not limiting. Although VPD and soil water are often correlated on a monthly to seasonal time scale, our results show the possible outcomes in the case of a heatwave occurring after or during a period of sustained precipitation. Disentangling the effects of VPD and T on plant hydraulics is of the utmost importance, as future T scenarios are well developed. Still, much more uncertainty exists on the air relative humidity. Therefore, predicting the effects of rising atmospheric evaporative demand on plants is challenging. Our findings highlight that VPD and T affect different hydraulic functions, hence having

differential consequences that are species-dependent. A prolonged but moderate increase in VPD and, to a certain extent, T led to hydraulic dysfunctions for *F. sylvatica* and *Q. pubescens* because of limited stomatal closure, higher transpiration, and more negative leaf water potentials. Whether these mechanisms are universal across a broad range of species remains to be tested as the relatively mild conditions used in this experiment were insufficient to induce significant xylem tensions for the xeric *Q. ilex* species. Although rising CO_2 levels are thought to possibly compensate for the adverse rising VPD effects by increasing the water use efficiency (Eamus 1991), uncertainties are significant, and further investigation into the interaction between VPD and CO_2 is needed. Nevertheless, our work emphasizes the importance of recognizing VPD and T as dominant drivers of plant functioning, both independently from each other and in interaction, to anticipate future impacts on ecosystems.

Acknowledgements

LS, CG, PS, and MML were supported by the Swiss National Science Foundation (P500PB_203127, PZ00P3_174068, and PZ00P2_179978). The Sandoz Family Foundation also supported CG. We thank Prof. Nina Buchmann and Hans-Jürg Lendi for their support and use of the climate chambers. We are thankful to Gary Perrenoud for his help with the µCT measurements.

References

Adams H.D., Guardiola-Claramonte M., Barron-Gafford G.A., Villegas J.C., Breshears D.D., Zou C.B., … Huxman T.E. (2009) Temperature sensitivity of drought-induced tree mortality portends increased regional die-off under global-change-type drought. *Proceedings of the National Academy of Sciences* **106**, 7063–7066.

Allen C.D., Breshears D.D. & McDowell N.G. (2015) On underestimation of global vulnerability to tree mortality and forest die-off from hotter drought in the Anthropocene. *Ecosphere* **6**.

Anderegg W.R.L. & Meinzer F.C. (2015) Wood anatomy and plant hydraulics in a changing climate. In *Functional and Ecological Xylem Anatomy*. (ed U. Hacke), pp. 235–253. Springer International Publishing, Cham.

Backes K. & Leuschner C. (2000) Leaf water relations of competitive *Fagus sylvatica* and *Quercus petraea* trees during 4 years differing in soil drought. *Canadian Journal of Forest Research* **30**, 335–346.

Barbero M., Loisel R. & Quézel P. (1992) Biogeography, ecology and history of Mediterranean *Quercus ilex* ecosystems. In *Quercus ilex L. ecosystems: function, dynamics and management*. (eds F.

524 Romane & J. Terradas), pp. 19–34. Springer Netherlands, Dordrecht.

525 Barron-Gafford G.A., Grieve K.A. & Murthy R. (2007) Leaf- and stand-level responses of a forested
526 mesocosm to independent manipulations of temperature and vapor pressure deficit. *New*
527 *Phytologist* **174**, 614–625.

528 Bartlett M.K., Klein T., Jansen S., Choat B. & Sack L. (2016) The correlations and sequence of plant
529 stomatal, hydraulic, and wilting responses to drought. *Proceedings of the National Academy of*
530 *Sciences* **113**, 13098–13103.

531 Bengtson C., Larsson S. & Liljenberg C. (1978) Effects of water stress on cuticular transpiration rate and
532 amount and composition of epicuticular wax in seedlings of six oat varieties. *Physiologia Plantarum*
533 **44**, 319–324.

534 Berry J. & Bjorkman O. (1980) Photosynthetic response and adaptation to temperature in higher plants.
535 *Annual Review of Plant Physiology* **31**, 491–543.

536 Buckley T.N. (2005) The control of stomata by water balance. *New Phytologist* **168**, 275–292.

537 Burkhardt J. & Pariyar S. (2016) How does the VPD response of isohydric and anisohydric plants depend
538 on leaf surface particles? *Plant Biology* **18**, 91–100.

539 Cardoso A.A., Brodribb T.J., Kane C.N., DaMatta F.M. & McAdam S.A.M. (2020) Osmotic adjustment and
540 hormonal regulation of stomatal responses to vapour pressure deficit in sunflower. *AoB PLANTS*
541 **12**.

542 Čater M. & Kobler A. (2017) Light response of Fagus sylvatica L. and Abies alba Mill. in different
543 categories of forest edge – Vertical abundance in two silvicultural systems. *Forest Ecology and*
544 *Management* **391**, 417–426.

545 Ciais P., Reichstein M., Viovy N., Granier A., Ogée J., Allard V., … Valentini R. (2005) Europe-wide
546 reduction in primary productivity caused by the heat and drought in 2003. *Nature* **437**, 529–533.

547 Cochard H. (2019) A new mechanism for tree mortality due to drought and heatwaves. *bioRxiv*, 531632.

548 Cochard H., Bodet C., Améglio T. & Cruiziat P. (2000a) Cryo-scanning electron microscopy observations
549 of vessel content during transpiration in walnut petioles. Facts or artifacts? *Plant Physiology* **124**,
550 1191–1202.

Cochard H., Martin R., Gross P. & Bogeat-Triboulot M.B. (2000b) Temperature effects on hydraulic conductance and water relations of *Quercus robur* L. *Journal of Experimental Botany* **51**, 1255–1259.

Daas C., Montpied P., Hanchi B. & Dreyer E. (2008) Responses of photosynthesis to high temperatures in oak saplings assessed by chlorophyll-a fluorescence: inter-specific diversity and temperature-induced plasticity. *Annals of Forest Science* **65**, 305.

Dai A. (2006) Recent climatology, variability, and trends in global surface humidity. *Journal of Climate* **19**, 3589–3606.

Dittmar C., Zech W. & Elling W. (2003) Growth variations of Common beech (*Fagus sylvatica* L.) under different climatic and environmental conditions in Europe—a dendroecological study. *Forest Ecology and Management* **173**, 63–78.

Drake J.E., Tjoelker M.G., Vårhammar A., Medlyn B.E., Reich P.B., Leigh A., … Barton C.V.M. (2018) Trees tolerate an extreme heatwave via sustained transpirational cooling and increased leaf thermal tolerance. *Global Change Biology* **24**, 2390–2402.

Duursma R.A., Blackman C.J., Lopéz R., Martin-StPaul N.K., Cochard H., Medlyn B.E., … Medlyn B.E. (2019) On the minimum leaf conductance: its role in models of plant water use, and ecological and environmental controls. *New Phytologist* **221**, 693–705.

Eamus D. (1991) The interaction of rising CO_2 and temperatures with water use efficiency. *Plant, Cell & Environment* **14**, 843–852.

Eamus D., Boulain N., Cleverly J. & Breshears D.D. (2013) Global change-type drought-induced tree mortality: vapor pressure deficit is more important than temperature per se in causing decline in tree health. *Ecology and Evolution* **3**, 2711–2729.

Fanourakis D., Heuvelink E. & Carvalho S.M.P. (2013) A comprehensive analysis of the physiological and anatomical components involved in higher water loss rates after leaf development at high humidity. *Journal of Plant Physiology* **170**, 890–898.

Fontes C.G., Dawson T.E., Jardine K., McDowell N., Gimenez B.O., Anderegg L., … Chambers J.Q. (2018) Dry and hot: the hydraulic consequences of a climate change-type drought for Amazonian trees. *Philosophical Transactions of the Royal Society B: Biological Sciences* **373**, 20180209.

579 Fu Z., Ciais P., Bastos A., Stoy P.C., Yang H., Green J.K., … Koebsch F. (2020) Sensitivity of gross primary
580 productivity to climatic drivers during the summer drought of 2018 in Europe. *Philosophical*
581 *Transactions of the Royal Society B: Biological Sciences* **375**, 20190747.

582 García-Plazaola J.I., Artetxe U. & Becerril J.M. (1999) Diurnal changes in antioxidant and carotenoid
583 composition in the Mediterranean schlerophyll tree *Quercus ilex* (L) during winter. *Plant Science*
584 **143**, 125–133.

585 Gardingen P.R. VAN & Grace J. (1992) Vapour pressure deficit response of cuticular conductance in
586 intact leaves of *Fagus sylvatica* L. *Journal of Experimental Botany* **43**, 1293–1299.

587 Geßler A., Keitel C., Nahm M. & Rennenberg H. (2004) Water shortage affects the water and nitrogen
588 balance in Central European beech forests. *Plant Biol (Stuttg)* **6**, 289–298.

589 Gimeno T.E., Pías B., Lemos-Filho J.P. & Valladares F. (2009) Plasticity and stress tolerance override local
590 adaptation in the responses of Mediterranean holm oak seedlings to drought and cold. *Tree*
591 *Physiology* **29**, 87–98.

592 Grossiord C., Buckley T.N., Cernusak L.A., Novick K.A., Poulter B., Siegwolf R.T.W., … McDowell N.G.
593 (2020a) Plant responses to rising vapor pressure deficit. *New Phytologist* **226**, 1550–1566.

594 Grossiord C., Gessler A., Reed S.C., Borrego I., Collins A.D., Dickman L.T., … McDowell N.G. (2018)
595 Reductions in tree performance during hotter droughts are mitigated by shifts in nitrogen cycling.
596 *Plant, Cell & Environment* **41**, 2627–2637.

597 Grossiord C., Ulrich D.E.M. & Vilagrosa A. (2020b) Controls of the hydraulic safety–efficiency trade-off.
598 *Tree Physiology* **40**, 573–576.

599 Gullo M.A. Lo & Salleo S. (1990) Wood anatomy of some trees with diffuse- and ring-porous wood: Some
600 functional and ecological interpretations. *Giornale botanico italiano* **124**, 601–613.

601 Hacke U. & Sauter J.J. (1996) Xylem dysfunction during winter and recovery of hydraulic conductivity in
602 diffuse-porous and ring-porous trees. *Oecologia* **105**, 435–439.

603 Haldimann P. & Feller U. (2004) Inhibition of photosynthesis by high temperature in oak (*Quercus*
604 *pubescens* L.) leaves grown under natural conditions closely correlates with a reversible heat-
605 dependent reduction of the activation state of ribulose-1,5-bisphosphate carboxylase/oxyg. *Plant,*
606 *Cell & Environment* **27**, 1169–1183.

607 Hoch G., Popp M. & Körner C. (2002) Altitudinal increase of mobile carbon pools in *Pinus cembra*
608 suggests sink limitation of growth at the Swiss treeline. *Oikos* **3**, 361–374.

609 Hochberg U., Windt C.W., Ponomarenko A., Zhang Y.J., Gersony J., Rockwell F.E. & Holbrook N.M. (2017)
610 Stomatal Closure, Basal Leaf Embolism, and Shedding Protect the Hydraulic Integrity of Grape
611 Stems. *Plant Physiology* **174**, 764–775.

612 IPCC (2021) *Climate Change 2021: The Physical Science Basis. Contribution of Working Group I to the*
613 *Sixth Assessment Report of the Intergovernmental Panel on Climate Change. (eds V. Masson-*
614 *Delmotte, P. Zhai, A. Pirani, S.L. Connors, C. Péan, S. Berger, N. Caud, Y. Ch*. Cambridge, UK and New
615 York, NY, USA: Cambridge University Press.

616 Jarvis P.G. & McNaughton K.G. (1986) Stomatal control of transpiration: scaling up from leaf to region.
617 *Advances in Ecological Research* **15**, 1–49.

618 Kerstiens G. (1996) Cuticular water permeability and its physiological significance. *Journal of*
619 *Experimental Botany* **47**, 1813–1832.

620 Knight C.A. & Ackerly D.D. (2002) An ecological and evolutionary analysis of photosynthetic
621 thermotolerance using the temperature-dependent increase in fluorescence. *Oecologia* **130**, 505–
622 514.

623 Koide R.T., Robichaux R.H., Morse S.R. & Smith C.M. (2000) Plant water status, hydraulic resistance and
624 capacitance. In *Plant Physiological Ecology: Field Methods and Instrumentation*. pp. 161–183.
625 Springer Netherlands, Dordrecht.

626 Lendzion J. & Leuschner C. (2008) Growth of European beech (*Fagus sylvatica* L.) saplings is limited by
627 elevated atmospheric vapour pressure deficits. *Forest Ecology and Management* **256**, 648–655.

628 Lens F., Sperry J.S., Christman M.A., Choat B., Rabaey D. & Jansen S. (2011) Testing hypotheses that link
629 wood anatomy to cavitation resistance and hydraulic conductivity in the genus Acer. *The New*
630 *phytologist* **190**, 709–723.

631 Liu L., Gudmundsson L., Hauser M., Qin D., Li S. & Seneviratne S.I. (2020) Soil moisture dominates
632 dryness stress on ecosystem production globally. *Nature Communications* **11**, 4892.

633 Martínez-Vilalta J., Poyatos R., Aguadé D., Retana J. & Mencuccini M. (2014) A new look at water
634 transport regulation in plants. *New Phytologist* **204**, 105–115.

635 McAdam S.A.M. & Brodribb T.J. (2016) Linking turgor with ABA biosynthesis: Implications for stomatal
636 responses to vapor pressure deficit across land plants. *Plant Physiology* **171**, 2008–2016.

637 Meyer B.F., Buras A., Rammig A. & Zang C.S. (2020) Higher susceptibility of beech to drought in
638 comparison to oak. *Dendrochronologia* **64**, 125780.

639 Monteith J.L. (1995) A reinterpretation of stomatal responses to humidity. *Plant, Cell and Environment*
640 **18**, 357–364.

641 Monteith J.L. & Unsworth M.H. (2013) *Principles of Environmental Physics*. Elsevier.

642 Nolf M., Lopez R., Peters J.M.R., Flavel R.J., Koloadin L.S., Young I.M. & Choat B. (2017) Visualization of
643 xylem embolism by X-ray microtomography: a direct test against hydraulic measurements. *New*
644 *Phytologist* **214**, 890–898.

645 Novick K.A., Ficklin D.L., Stoy P.C., Williams C.A., Bohrer G., Oishi A.C., … Phillips R.P. (2016) The
646 increasing importance of atmospheric demand for ecosystem water and carbon fluxes. *Nature*
647 *Climate Change* **6**, 1023–1027.

648 Olson M.E., Anfodillo T., Rosell J.A. & Martínez-Méndez N. (2020) Across climates and species, higher
649 vapour pressure deficit is associated with wider vessels for plants of the same height. *Plant, Cell &*
650 *Environment* **43**, 3068–3080.

651 Oren R., Sperry J.S., Katul G.G., Pataki D.E., Ewers B.E., Phillips N. & Schäfer K.V.R. (1999) Survey and
652 synthesis of intra- and interspecific variation in stomatal sensitivity to vapour pressure deficit.
653 *Plant, Cell & Environment* **22**, 1515–1526.

654 Pearcy R.W., E.-D S. & Zimmermann R. (2000) Measurement of transpiration and leaf conductance. In
655 *Plant Physiological Ecology: Field Methods and Instrumentation*. (eds R.W. Pearcy, J.R. Ehleringer,
656 H.A. Mooney & P.. Rundel), pp. 137–160. Kluwer Academic, Dordrecht, The Netherlands.

657 Pena-Rojas K., Aranda X. & Fleck I. (2004) Stomatal limitation to CO_2 assimilation and down-regulation of
658 photosynthesis in *Quercus ilex* resprouts in response to slowly imposed drought. *Tree Physiology*
659 **24**, 813–822.

660 Petersson L.K., Löf M., Jensen A.M., Chastain D.R. & Gardiner E.S. (2020) Sprouts of shoot-clipped oak
661 (Quercus alba and Q. robur) germinants show morphological and photosynthetic acclimation to
662 contrasting light environments. *New Forests* **51**, 817–834.

663 Pflug E.E., Buchmann N., Siegwolf R.T.W., Schaub M., Rigling A. & Arend M. (2018) Resilient leaf
664 physiological response of European beech (Fagus sylvatica L.) to summer drought and drought
665 release. *Frontiers in Plant Science* **9**, 1–11.

666 Quentin A.G., Pinkard E.A., Ryan M.G., Tissue D.T., Baggett L.S., Adams H.D., … Woodruff D.R. (2015)
667 Non-structural carbohydrates in woody plants compared among laboratories. *Tree Physiology* **35**,
668 1146–1165.

669 Rehschuh R., Rehschuh S., Gast A., Jakab A.-L., Lehmann M.M., Saurer M., … Ruehr N.K. (2021) Tree
670 allocation dynamics beyond heat and hot drought stress reveal changes in carbon storage,
671 belowground translocation and growth. *New Phytologist* **233**, 687–704.

672 Schipka F., Heimann J. & Leuschner C. (2005) Regional variation in canopy transpiration of Central
673 European beech forests. *Oecologia* **143**, 260–270.

674 Schleppi P. (2021) Pixstat. *https://www.schleppi.ch/pixstat/*.

675 Schönbeck L., Gessler A., Hoch G., McDowell N.G., Rigling A., Schaub M. & Li M.H. (2018) Homeostatic
676 levels of nonstructural carbohydrates after 13 yr of drought and irrigation in *Pinus sylvestris*. *New*
677 *Phytologist* **219**, 1314–1324.

678 Schuster A.-C. (2016) Chemical and functional analyses of the plant cuticle as leaf transpiration barrier.

679 Schuster A.-C., Burghardt M., Alfarhan A., Bueno A., Hedrich R., Leide J., … Riederer M. (2016)
680 Effectiveness of cuticular transpiration barriers in a desert plant at controlling water loss at high
681 temperatures. *AoB PLANTS* **8**.

682 Schuster A.-C., Burghardt M. & Riederer M. (2017) The ecophysiology of leaf cuticular transpiration: are
683 cuticular water permeabilities adapted to ecological conditions? *Journal of Experimental Botany*
684 **68**, 5271–5279.

685 Seemann J.R., Berry J.A. & Downton W.J.S. (1984) Photosynthetic response and adaptation to high
686 temperature in desert plants 1: A comparison of gas exchange and fluorescence methods for
687 studies of thermal tolerance. *Plant Physiology* **75**, 364–368.

688 Senf C. & Seidl R. (2021) Persistent impacts of the 2018 drought on forest disturbance regimes in
689 Europe. *Biogeosciences* **18**, 5223–5230.

690 Sermons S.M., Seversike T.M., Sinclair T.R., Fiscus E.L. & Rufty T.W. (2012) Temperature influences the

691 ability of tall fescue to control transpiration in response to atmospheric vapour pressure deficit.
692 *Functional Plant Biology* **39**, 979–986.

693 Sperry J.S., Donnelly J.R. & Tyree M.T. (1988) A method for measuring hydraulic conductivity and
694 embolism in xylem. *Plant, Cell and Environment* **11**, 35–40.

695 Staudt M., Joffre R. & Rambal S. (2003) How growth conditions affect the capacity of Quercus ilex leaves
696 to emit monoterpenes. *New Phytologist* **158**, 61–73.

697 Tardieu F. & Simonneau T. (1998) Variability among species of stomatal control under fluctuating soil
698 water status and evaporative demand: modelling isohydric and anisohydric behaviours. *Journal of*
699 *Experimental Botany* **49**, 419–432.

700 Thomas F.M. (2000) Growth and water relations of four deciduous tree species (Fagus sylvatica L.,
701 Quercus petraea [MATT.] LIEBL., Q-pubescens WILLD., Sorbus aria [L.] CR.) occurring at Central-
702 European tree-line sites on shallow calcareous soils: physiological reactions of . *Flora* **195**, 104–
703 115.

704 Tixier A., Herbette S., Jansen S., Capron M., Tordjeman P., Cochard H. & Badel E. (2014) Modelling the
705 mechanical behaviour of pit membranes in bordered pits with respect to cavitation resistance in
706 angiosperms. *Annals of botany* **114**, 325–334.

707 Tognetti R., Longobucco A., Miglietta F. & Raschi A. (1998a) Transpiration and stomatal behaviour of
708 *Quercus ilex* plants during the summer in a Mediterranean carbon dioxide spring. *Plant, Cell and*
709 *Environment* **21**, 613–622.

710 Tognetti R., Longobucco A. & Raschi A. (1998b) Vulnerability of xylem to embolism in relation to plant
711 Hhdraulic resistance in Quercus pubescens and Quercus ilex co-occurring in a Mediterranean
712 coppice stand in Central Italy. *The New Phytologist* **139**, 437–447.

713 Trotsiuk V., Babst F., Grossiord C., Gessler A., Forrester D.I., Buchmann N., … Eugster W. (2021) Tree
714 growth in Switzerland is increasingly constrained by rising evaporative demand. *Journal of Ecology*
715 **109**, 2981–2990.

716 Urban J., Ingwers M.W., McGuire M.A. & Teskey R.O. (2017) Increase in leaf temperature opens stomata
717 and decouples net photosynthesis from stomatal conductance in Pinus taeda and Populus
718 deltoides x nigra. *Journal of Experimental Botany* **68**, 1757–1767.

719 Walthert L., Ganthaler A., Mayr S., Saurer M., Waldner P., Walser M., … von Arx G. (2021) From the
720 comfort zone to crown dieback: Sequence of physiological stress thresholds in mature European
721 beech trees across progressive drought. *Science of The Total Environment* **753**, 141792.

722 Wellstein C. & Spada F. (2015) The Status of Quercus pubescens Willd. in Europe. In *Warm-Temperate*
723 *Deciduous Forests around the Northern Hemisphere*. (eds E.O. Box & K. Fujiwara), pp. 153–163.
724 Springer International Publishing, Cham.

725 Wong S.C. (1990) Elevated atmospheric partial pressure of CO2 and plant growth - II. Non-structural
726 carbohydrate content in cotton plants and its effect on growth parameters. *Photosynthesis*
727 *Research* **23**, 171–180.

728 Yang Y., Zhang Q., Huang G., Peng S. & Li Y. (2020) Temperature responses of photosynthesis and leaf
729 hydraulic conductance in rice and wheat. *Plant, Cell & Environment* **43**, pce.13743.

730 Zhu J., Thimonier A., Etzold S., Meusburger K., Waldner P., Schmitt M., … Lehmann M.M. (2022)
731 Variation in leaf morphological traits of European beech and Norway spruce over two decades in
732 Switzerland. *Frontiers in Forests and Global Change* **4**.

733

Figure legends

Figure 1. Average temperature and VPD in the six climate chambers. Plants were exposed to two temperature treatments (25°C and 30°C) and three VPD levels that are defined by low (L), middle (M) and high (H) VPD. Symbols indicate the average (± SD) over the total treatment period (June 1st – November 8th, 2020).

Figure 2. Micro-computed tomography images of stem sections of *Fagus sylvatica* (a, b), *Quercus pubescens* (c, d), and *Quercus ilex* (e, f) on the intact stems (a, c, e) and after flushing the stem segments with air at high pressure (b, d, f). Black areas indicate air-filled vessels. Grey areas indicate wood and water-filled sections. The red circles indicate the area of interest, including only the xylem and excluding bark and phloem. Percent loss of conductive area (PLA) was calculated as embolized vessel area / total vessel area x 100%.

Figure 3. Relationship between the percentage loss of conductive area (PLA, %), measured using micro-computed tomography, and the percentage loss of conductivity (PLC, %), calculated using hydraulic conductivity measurements. Symbols indicate species and colors indicate temperature and VPD treatments. The dashed grey line indicates the 1:1 ratio. The black line indicates the fitted regression line. Confidence interval of the slope was 0.65 – 1.05, indicating no significant deviation from the 1:1 line.

Figure 4. Percentage loss of conductive area, calculated as the change in PLA from the start of the experiment (dPLA, %total embolized - %embolized at campaign 1), percentage loss of conductivity (PLC) and midday leaf water potential ($\psi_{leaf,md}$) in *Fagus sylvatica, Quercus pubescens* and *Quercus ilex* in the two temperature and three VPD treatments. Data are shown in relation to the average VPD in the chambers during the treatment period. Symbols indicate the mean ± SE of the three measurement campaigns (n = 18), except for PLC which was measured once at the end of the experiment (n = 6). Dashed lines indicate significant VPD effects without temperature effects. Colored lines – blue for 25°C and red for 30°C – indicate an additive (T x VPD: ns) or interacting (T x VPD: $p < 0.05$) temperature effect in addition to VPD.

Figure 5. Transpiration (E), stomatal conductance (g_s), minimum leaf conductance (g_{min}), sensitivity of g_s to VPD (m) and turgor loss point (ψ_{TLP}) in *Fagus sylvatica, Quercus pubescens* and *Quercus Ilex* in the two temperature and three VPD treatments. Data are shown in relation to the average VPD in the chambers during the treatment period. Symbols indicate the mean ± SE of three measurement campaigns (n = 18). Dashed lines indicate significant VPD effects without temperature effects. Colored lines – blue for 25°C and red for 30°C – indicate the VPD effects in the separate temperature treatments in case of a T x VPD interaction. In case of absence of a VPD effect, temperature effects are indicated with asterisks (*: $p < 0.05$; **: $p < 0.01$; ***: $p < 0.001$).

Figure 6. Correlation analysis of PLA with stomatal conductance (g_s), minimum leaf conductance (g_{min}), maximum hydraulic conductance of the stem (K_{max}), water potential of the leaf at midday ($\psi_{leaf,md}$) and sugar concentrations in the leaves. Colored lines indicate significant correlations within the corresponding temperature treatment (blue for 25°C and red for 30°C). Analyses were done with all species pooled.

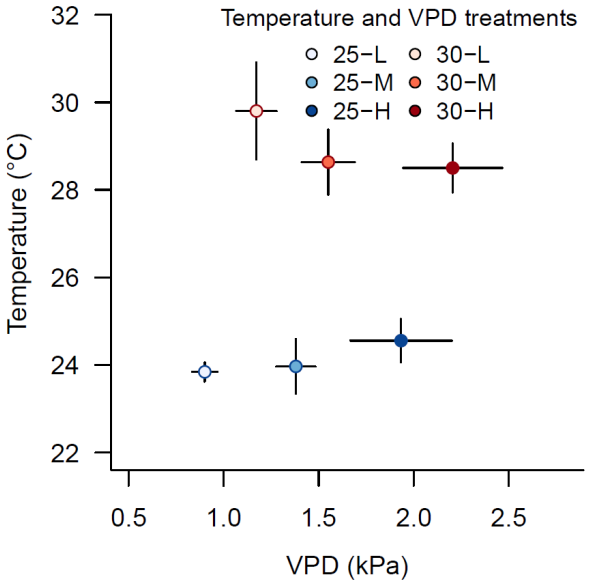

771

772 **Figure 1.** Average temperature and VPD in the six climate chambers. Plants were exposed to two
773 temperature treatments (25°C and 30°C) and three VPD levels that are defined by low (L), middle (M) and
774 high (H) VPD. Symbols indicate the average (± SD) over the total treatment period (June 1st – November
775 8th, 2020).

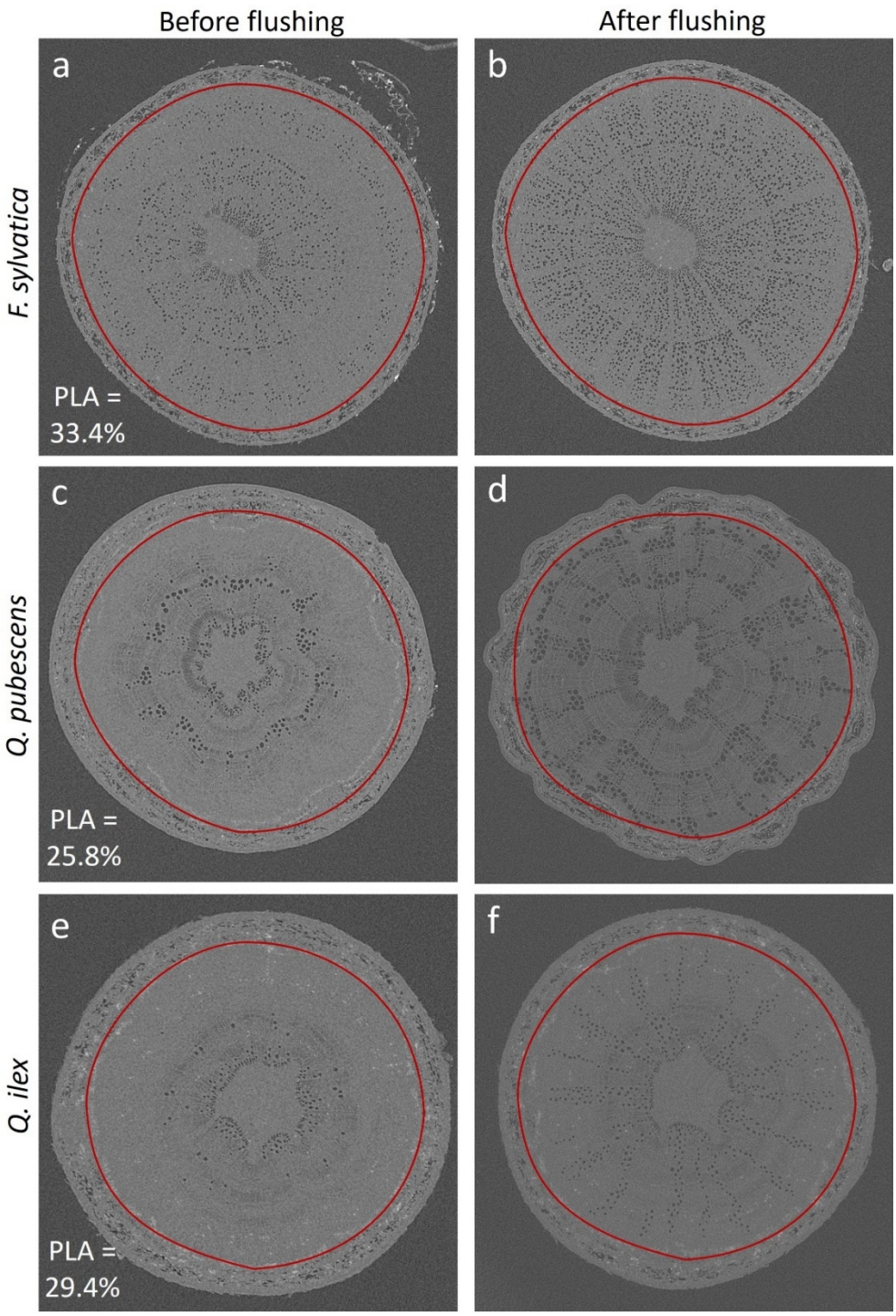

Figure 2. Micro-computed tomography images of stem sections of *Fagus sylvatica* (a, b), *Quercus pubescens* (c, d), and *Quercus ilex* (e, f) on the intact stems (a, c, e) and after flushing the stem segments with air at high pressure (b, d, f). Black areas indicate air-filled vessels. Grey areas indicate wood and water-filled sections. The red circles indicate the area of interest, including only the xylem and excluding bark and phloem. Percent loss of conductive area (PLA) was calculated as embolized vessel area / total vessel area x 100%.

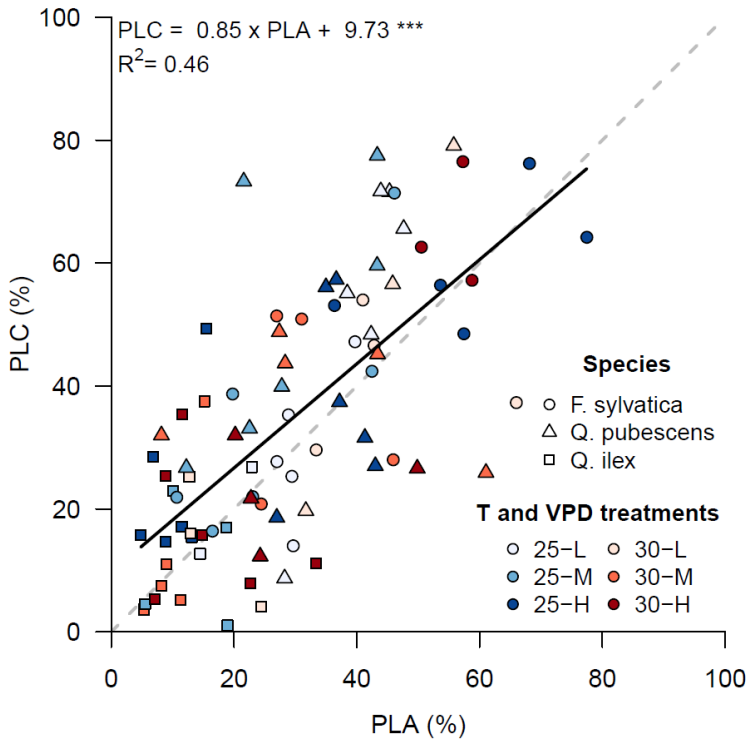

783

784 **Figure 3.** Relationship between the percentage loss of conductive area (PLA, %), measured using micro-
785 computed tomography, and the percentage loss of conductivity (PLC, %), calculated using hydraulic
786 conductivity measurements. Symbols indicate species and colors indicate temperature and VPD
787 treatments. The dashed grey line indicates the 1:1 ratio. The black line indicates the fitted regression line.
788 Confidence interval of the slope was 0.65 – 1.05, indicating no significant deviation from the 1:1 line.

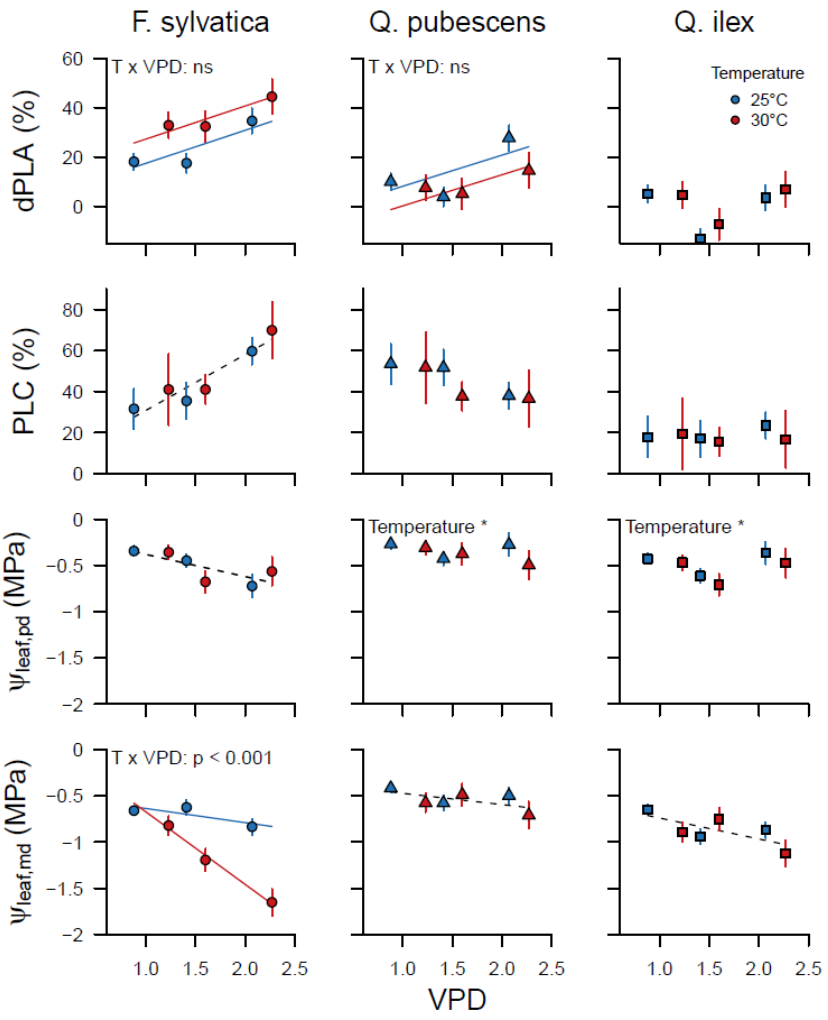

789

790 **Figure 4.** Percentage loss of conductive area, calculated as the change in PLA from the start of the
791 experiment (dPLA, %total 2dembolized - %embolized at campaign 1), percentage loss of conductivity (PLC)
792 and predawn and midday leaf water potential ($\psi_{leaf,pd}$ & $\psi_{leaf,md}$) in *Fagus sylvatica, Quercus pubescens* and
793 *Quercus ilex* in the two temperature and three VPD treatments. Data are shown in relation to the average
794 VPD in the chambers during the treatment period. Symbols indicate the mean ± SE of the three
795 measurement campaigns (n = 18), except for PLC which was measured once at the end of the experiment
796 (n = 6). Dashed lines indicate significant VPD effects without temperature effects. Colored lines – blue for
797 25°C and red for 30°C – indicate an additive (T x VPD: ns) or interacting (T x VPD: $p < 0.05$) temperature
798 effect in addition to VPD.

799

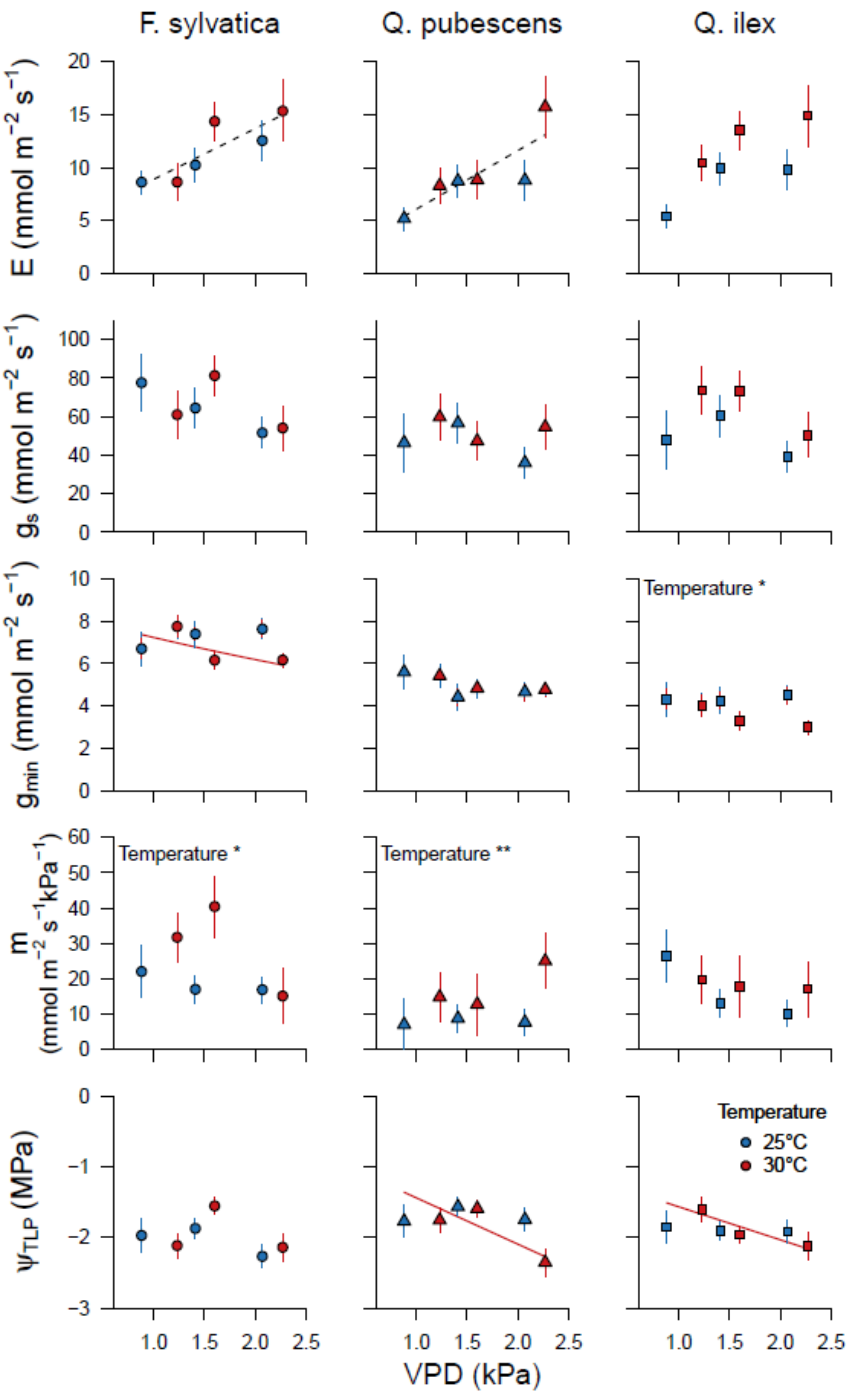

Figure 5. Transpiration (E), stomatal conductance (g_s), minimum leaf conductance (g_{min}), sensitivity of g_s to VPD (m) and turgor loss point (ψ_{TLP}) in *Fagus sylvatica, Quercus pubescens* and *Quercus Ilex* in the two temperature and three VPD treatments. Data are shown in relation to the average VPD in the chambers during the treatment period. Symbols indicate the mean ± SE of three measurement campaigns (n = 18). Dashed lines indicate significant VPD effects without temperature effects. Colored lines – blue for 25°C and red for 30°C – indicate the VPD effects in the separate temperature treatments in case of a T x VPD interaction. In case of absence of a VPD effect, temperature effects are indicated with asterisks (*: $p < 0.05$; **: $p < 0.01$; ***: $p < 0.001$).

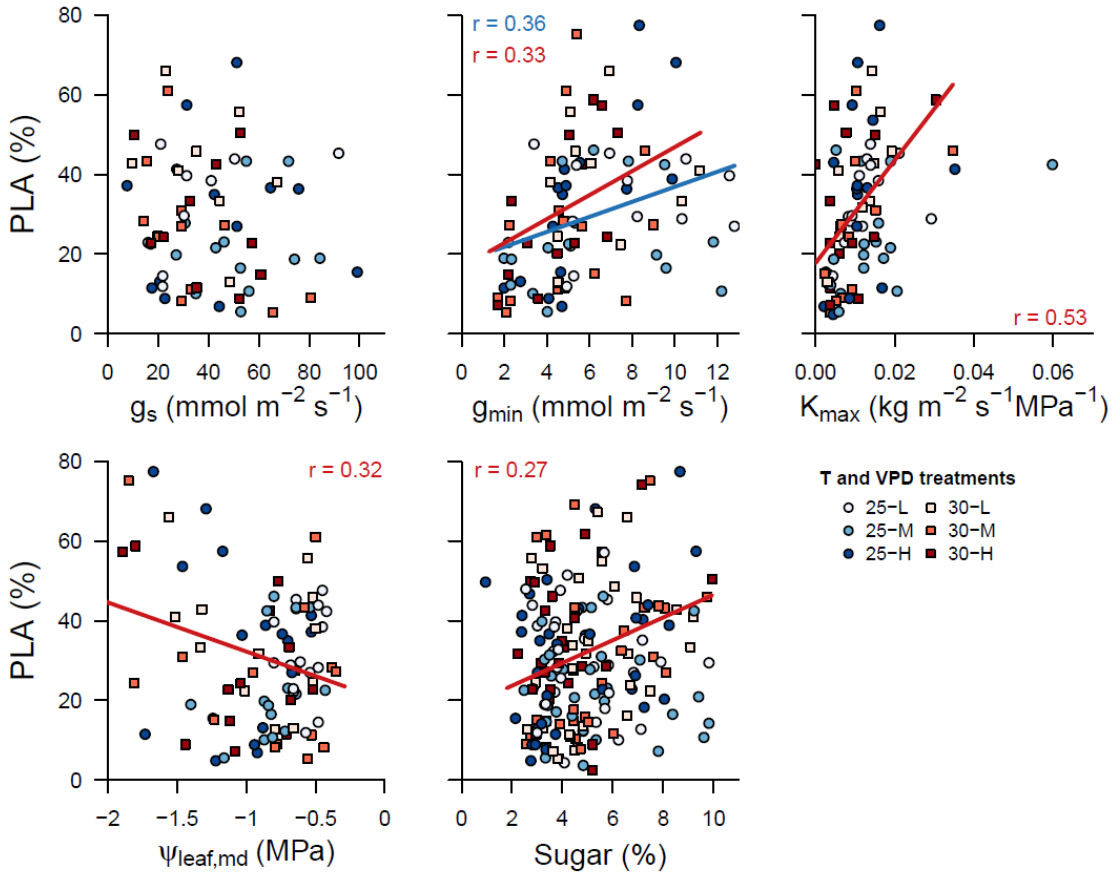

809

810 **Figure 6.** Correlation analysis of PLA with stomatal conductance (g_s), minimum leaf conductance (g_{min}),
811 maximum hydraulic conductance of the stem (K_{max}), water potential of the leaf at midday ($\psi_{leaf,md}$) and
812 sugar concentrations in the leaves. Colored lines indicate significant correlations within the corresponding
813 temperature treatment (blue for 25°C and red for 30°C). Analyses were done with all species pooled.